Dyes and Pigments 92 (2011) 517–523

Contents lists available at ScienceDirect

Dyes and Pigments

journal homepage: www.elsevier.com/locate/dyepig

Synthesis, photophysical and electrochemical properties of 1-aminoperylene bisimides

Kew-Yu Chen*, Tzu-Chien Fang, Ming-Jen Chang

Department of Chemical Engineering, Feng Chia University, 40724 Taichung, Taiwan, R.O.C

ARTICLE INFO

Article history:
Received 17 May 2011
Received in revised form
16 June 2011
Accepted 17 June 2011
Available online 29 June 2011

Keywords:
1-Aminoperylene bisimides
Intramolecular charge transfer
Purple dyes
Self-assembly

ABSTRACT

1-Aminoperylene bisimides (**1a**–**1c**) were synthesized under mild condition in high yields, and were characterized by FT-IR, ^{1}H NMR, UV–Vis, HRMS spectra, cyclic voltammetry, differential scanning calorimetry, and thermogravimetric analyses. These compounds are stable up to 310 °C according to thermogravimetric analyses. They undergo two quasi-reversible one-electron oxidations and two quasi-reversible one-electron reductions in dichloromethane at modest potentials. Their spectroscopic properties in various conditions and complementary density functional theory (DFT) calculations are reported.

1. Introduction

Derivatives of perylene-3,4:9,10-bis(dicarboximide) (PDI) have attracted considerable attention due to their applications in molecular electronic devices, such as photovoltaic cells [1–8], light-harvesting arrays [9,10], light-emitting diodes [11], organic field-effect transistors (OFETs) [12–17], photochromic materials [18], and LCD color filters [19]. These chromophores are advantageous due to their high photochemical stability, ease of synthetic modification and reversible redox properties. Moreover, the electronic characteristics of PDI can be fine-tuned by the substitution of the conjugated aromatic core. Many perylene bisimide derivatives with either electron-donating or electron-withdrawing groups have been reported in the literature, such as (a) pyrrolidinyl-substituted perylene bisimides [20], (b) piperidinyl-substituted perylene bisimides [21], (c) alkoxy-substituted perylene bisimides [22], (d) aryl-substituted perylene bisimides [23], (e) cyano-substituted perylene bisimides [24], (f) nitro-substituted perylene bisimides [25], etc. Furthermore, perylene bisimides modified with electron-donating groups have been characterized as near-infrared fluorescent dyes [26], and some with strong electron-withdrawing groups have been used as air-stable *n*-type organic semiconductors [27,28]. To date, a promising strategy for introducing substituents onto the PDI core is chlorination or bromination of perylene dianhydride [29]. Replacement of these halogens is readily achieved by traditional substitution reactions or by metal-catalyzed cross-coupling reactions [30]. However, both of these methods are usually accompanied by stringent reaction conditions such as high temperatures, and absence of water and oxygen. More recently, alkyl amino-substituted perylene bisimides have been synthesized based on the above methods, and have been characterized as new photoactive charge transport materials and as stable near-infrared fluorescent dyes [31]. To expand the scope of chromophores available for designing systems for self-assembly and colorful dyes based on PDI, we have synthesized a series of amino-substituted perylene bisimides, since previous studies have used either flexible alkyl (**DAPER3C**) [32] or sterically bulky cyclic amines (**5b**–**5c**) [33] as electron-donating groups (Fig. 1). These chromophores (**5b**–**5c** and **DAPER3C**) show green or blue colors, both in the solid form and in solution. We now report on the introduction of an amino group of PDI affording chromophores that are intense purple in color and that readily undergo two quasi-reversible one-electron oxidations and two quasi-reversible one-electron reductions.

2. Experimental

2.1. Chemicals and instruments

All reagents such as perylene-3,4,9,10-tetracarboxyldianhydride, cyclohexylamine, octylamine, butylamine, acetic acid, cerium (IV) ammonium nitrate (CAN), 1-methyl-2-pyrrolidinone (NMP), and tin (II) chloride dihydrate ($SnCl_2 \cdot 2H_2O$) were purchased from Aldrich

* Corresponding author. Tel.: +886 4 24517250x3683; fax: +886 4 24510890.
E-mail address: kyuchen@fcu.edu.tw (K.-Y. Chen).

0143-7208/$ – see front matter © 2011 Elsevier Ltd. All rights reserved.
doi:10.1016/j.dyepig.2011.06.023

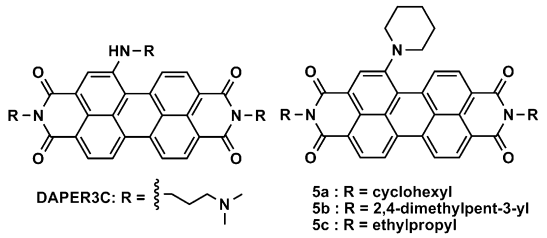

Fig. 1. The structures of alkylamino-substituted (**DAPER3C**) and bulky cyclic amino-substituted perylene bisimides (**5a**–**5c**).

Chemical Co.. These were used without further purification unless otherwise noted. Solvents were dried and purified by fractional distillation over sodium and handled in a moisture-free atmosphere. Column chromatography was performed using silica gel (Merk, 250–430 mesh).

^{1}H NMR spectra were recorded in $CDCl_3$ on a Varian Mercury 400 MHz. FT-IR spectra were measured with a Horiba FT-720 infrared spectrophotometer. Mass spectra were recorded on a VG70-250S mass spectrometer. The absorption and photoluminescence (PL) spectra were measured using a Jasco V-570 UV–Vis spectrometer and a Hitachi F-4500 fluorescence spectrometer, respectively. Cyclic voltammetry (CV) was carried out with a CH instruments (Electrochemical Workstation) at a potential rate of 200 mV/s in a 0.1 M solution of tetrabutylammonium hexafluorophosphate ($TBAPF_6$) in dichloromethane. A platinum wire was used as the counter electrode and an $Ag/AgNO_3$ electrode was used as the reference electrode. Thermogravimetric analysis (TGA) was conducted under nitrogen at a heating rate of 10 °C/min with a TA Instruments Thermogravimetric Analyzer 2050.

2.2. Synthesis and characterization

2.2.1. General procedure for nitration

3a (**3b** or **3c**) (1.8 mmol), cerium (IV) ammonium nitrate (CAN) (1.2 g, 2.2 mmol), nitric acid (2.0 g, 31.7 mmol) and dichloromethane

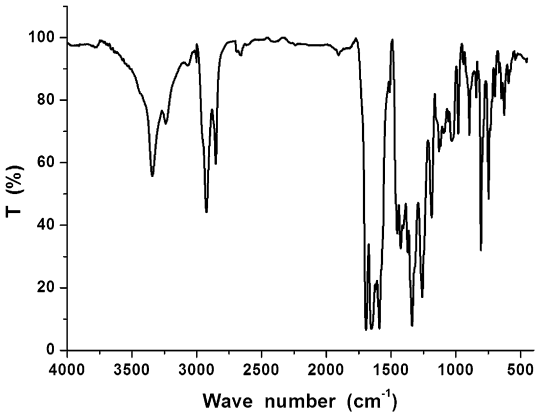

Fig. 2. FT-IR spectra of **1a**.

(150 mL) were stirred at 25 °C under N_2 for 2 h. The mixture was neutralized with 10% KOH and extracted with CH_2Cl_2. After solvent was removed, the crude product was purified by silica gel column chromatography with eluent CH_2Cl_2 to afford **2a** (**2b** or **2c**) in 95% yield. Characterization data: **2a**: ^{1}H NMR (400 MHz, $CDCl_3$) δ 8.74 (d, J = 7.6 Hz, 1H), 8.62–8.69 (m, 4H), 8.55 (d, J = 8.0 Hz, 1H), 8.18 (d, J = 7.6 Hz, 1H), 5.00 (m, 2H), 2.54 (m, 4H), 1.91 (m, 4H), 1.76 (m, 6H), 1.47 (m, 4H), 1.34 (m, 2H); IR (KBr): 2928, 2851, 1700, 1659, 1596, 1539, 1401, 1336, 1262, 1245, 1190, 809, 743 cm^{-1}; MS (FAB): m/z (relative intensity) 600 ($M + H^+$, 100); HRMS calcd. for $C_{36}H_{30}O_6N_3$ 600.2135, found 600.2141. Selected data for **2b**: ^{1}H NMR (400 MHz, $CDCl_3$) δ 8.79 (d, J = 8.0 Hz, 1H), 8.73–8.67 (m, 4H), 8.60 (d, J = 8.0 Hz, 1H), 8.23 (d, J = 8.0 Hz, 1H), 4.19 (m, 4H), 1.76 (m, 4H), 1.26–1.54 (m, 20H), 0.87 (t, J = 6.5 Hz, 6H); MS (FAB): m/z (relative intensity) 660 ($M + H^+$, 100); HRMS calcd. for $C_{40}H_{42}O_6N_3$ 660.3074, found 660.3076. Selected data for **2c**: ^{1}H NMR (400 MHz, $CDCl_3$) δ 8.80 (d, J = 8.0 Hz, 1H), 8.79–8.68 (m, 4H), 8.62 (d, J = 8.0 Hz, 1H), 8.25 (d, J = 8.0 Hz, 1H), 4.22 (m, 4H), 1.76 (m, 4H), 1.48 (m, 4H), 0.98 (t, J = 7.2 Hz, 6H); MS (FAB): m/z (relative intensity) 548 ($M + H^+$, 100); HRMS calcd. for $C_{32}H_{26}O_6N_3$ 548.1822, found 548.1826.

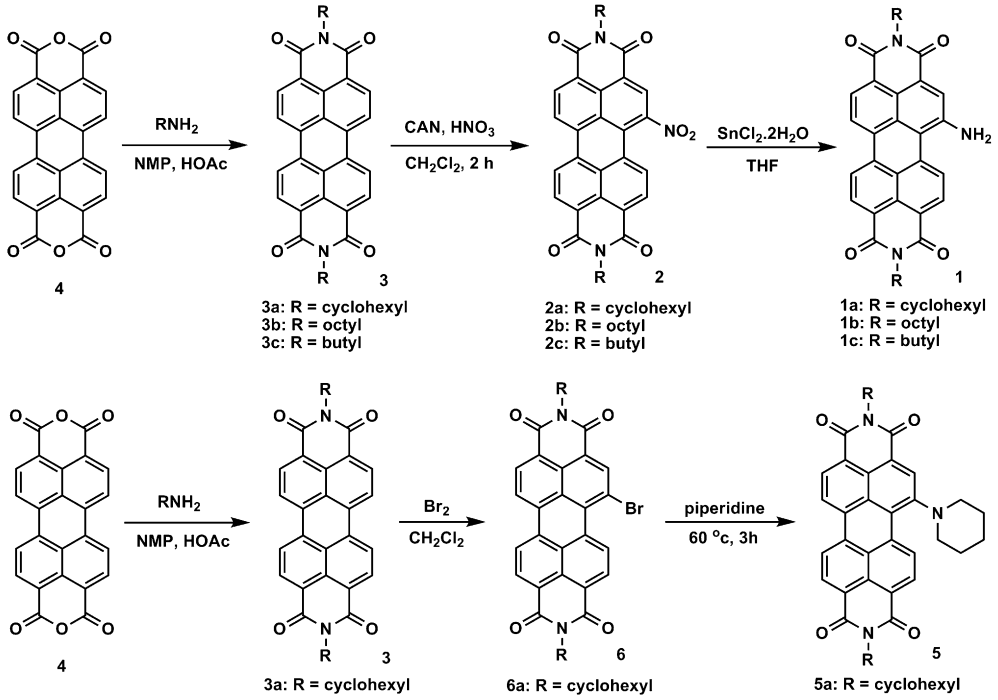

Scheme 1. The synthetic routes of **1a**–**1c** and **5a**.

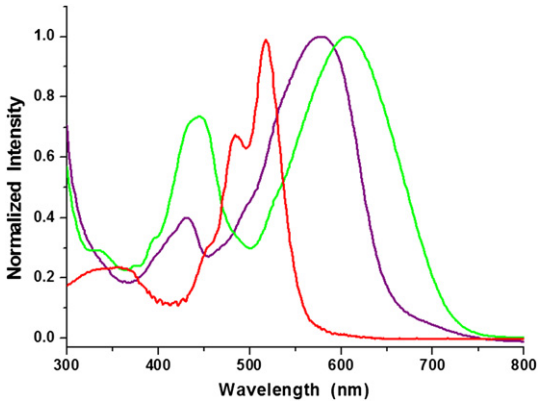

Fig. 3. Normalized absorption spectra of **1a** (purple line), **2a** (red line) and **5a** (green line) in dichloromethane solution.

2.2.2. General procedure for reduction

Tin chloride dihydrate (5.0 g, 22 mmol), and **2a** (**2b** or **2c**) (1.0 g, 1.7 mmol) were suspended in 50 mL of THF, and stirred 20 min. The solvent was refluxed 80 °C with stirring for 2 h. THF is removed at the rotary evaporator, and the residue was dissolved in ethyl acetate and washed with 10% sodium hydrate solution and brine. The organic layer was dried over anhydrous $MgSO_4$ and the filtrate was concentrated under reduced pressure. The crude product was purified by silica gel column chromatography with eluent ethyl acetate/*n*-hexane (2/3) to afford **1a** (**1b** or **1c**) in 80% yield. Characterization data: **1a**: ^{1}H NMR (400 MHz, $CDCl_3$) δ 8.62 (d, $J = 8.0$ Hz, 1H), 8.45 (d, $J = 7.6$ Hz, 1H), 8.38 (d, $J = 8.0$ Hz, 1H), 8.25 (d, $J = 7.6$ Hz, 1H), 8.18 (d, $J = 8.0$ Hz, 1H), 8.10 (d, $J = 8.0$ Hz, 1H), 7.98 (s, 1H), 5.03, (s, 2H), 4.99 (m, 2H), 2.55 (m, 4H), 1.91 (m, 4H), 1.74 (m, 6H), 1.46–1.40 (m, 6H); IR (KBr): 3346, 3240, 2926, 1694, 1653, 1372, 1338, 1260, 806, 747 cm^{-1}; MS (FAB): *m/z* (relative intensity) 570 ($M + H^+$, 100); HRMS calcd. for $C_{36}H_{32}O_4N_3$ 570.2393, found 570.2396. Elemental analysis: Calcd for $C_{36}H_{31}O_4N_3$: C, 75.90; H, 5.49; N, 7.38. Found C, 75.74; H, 5.57; N, 7.52. Selected data for **1b**: ^{1}H NMR (400 MHz, $CDCl_3$) δ 8.82 (d, $J = 8.0$ Hz, 1H), 8.62 (d, $J = 7.6$ Hz, 1H), 8.59 (d, $J = 8.0$ Hz, 1H), 8.49 (d, $J = 7.6$ Hz, 1H), 8.44 (d, $J = 8.0$ Hz, 1H), 8.41 (d, $J = 8.0$ Hz, 1H), 8.10 (s, 1H), 5.04, (s, 2H), 4.18 (m, 4H), 1.88 (m, 4H), 1.23–1.74 (m, 26H); MS (FAB): *m/z* (relative intensity) 630 ($M + H^+$, 100); HRMS calcd. for $C_{40}H_{44}O_4N_3$ 630.3332, found 630.3330. Elemental analysis: Calcd for $C_{40}H_{43}O_4N_3$: C, 76.28; H, 6.88; N, 6.67. Found C, 76.06; H, 6.96; N, 6.79. Selected data for **1c**: ^{1}H NMR (400 MHz, $CDCl_3$) δ 8.80 (d, $J = 8.0$ Hz, 1H), 8.74 (d, $J = 7.6$ Hz, 1H), 8.72 (d, $J = 8.0$ Hz, 1H), 8.70 (d, $J = 7.6$ Hz, 1H), 8.67 (d, $J = 8.0$ Hz, 1H), 8.59 (d, $J = 8.0$ Hz, 1H), 8.11 (s, 1H), 5.12, (s, 2H), 4.20 (m, 4H), 1.77 (m, 4H), 1.47 (m, 4H), 1.00 (t, $J = 7.2$ Hz, 6H); MS (FAB): *m/z* (relative intensity) 518 ($M + H^+$, 100); HRMS calcd. for $C_{32}H_{28}O_4N_3$ 518.2080, found 518.2084. Elemental analysis: Calcd for $C_{32}H_{27}O_4N_3$: C, 74.26; H, 5.26; N, 8.12. Found C, 74.08; H, 5.32; N, 8.28.

Table 1
Summary of optical absorption and emission properties of **1a** in various solvents.

Compound **1a**	λ_{abs} (nm)/(ε (M^{-1} cm^{-1})[a])	λ_{em} (nm)	Φ[b]
Cyclohexane	554	624	0.25
Ethyl acetate	571	663	0.16
Dichloromethane	578 (41 200)	677	0.10
Acetonitrile	581	690	0.06

[a] Measured at 2×10^{-5} M.
[b] Determined with *N,N′*-dioctyl-3,4,9,10-perylenedicarboximide as reference [36].

Table 2
Summary of optical absorption and emission properties of **5a** in various solvents.

Compound **5a**	λ_{abs} (nm)/(ε (M^{-1} cm^{-1})[a])	λ_{em} (nm)	Φ[b]
Cyclohexane	581	687	0.18
Ethyl acetate	595	722	0.11
Dichloromethane	599 (43 600)	731	0.06
Acetonitrile	607	748	0.04

[a] Measured at 2×10^{-5} M.
[b] Determined with *N,N′*-dioctyl-3,4,9,10-perylenedicarboximide as reference [36].

2.2.3. Synthesis of 1-(N-piperidyl)-N,N′-bis(cyclohexyl)-3,4:9,10-perylenebis(dicarboximide) (**5a**)

1-bromoperylene bisimide (**6a**) (500 mg, 7.9 mmol) [33] was dissolved in 50 mL piperidine. The solution was heated at 60 °C under nitrogen for 3 h with stirring. Excess piperidine was removed on a rotary evaporator and the residue was purified by silica gel column chromatography with dichloromethane/*n*-hexane (2/1) to afford **5a** (430 mg, 85%). Characterization data for **5a**: ^{1}H NMR (400 MHz, $CDCl_3$) δ 9.80 (d, $J = 8.0$ Hz, 1H), 8.61 (d, $J = 7.6$ Hz, 1H), 8.59 (d, $J = 7.6$ Hz, 1H), 8.53 (s, 1H), 8.46–8.49 (m, 3H), 5.07, (m, 2H), 3.44 (m, 2H), 2.93 (m, 2H), 2.55 (m, 4H), 1.74–1.90 (m, 14H), 1.20–1.46 (m, 8H); MS (FAB): *m/z* (relative intensity) 638 ($M + H^+$, 100); HRMS calcd. for $C_{41}H_{40}O_4N_3$ 638.3019, found 638.3016. Elemental analysis: Calcd for $C_{41}H_{39}O_4N_3$: C, 77.21; H, 6.16; N, 6.59. Found C, 77.35; H, 6.08; N, 6.43.

3. Results and discussion

3.1. Synthesis of dyes

Scheme 1 shows the chemical structures and synthetic routes of compounds **1a**–**1c** and **5a**. The synthesis starts from an imidization of perylene bisanhydride (**4**) by reaction with cyclohexylamine, octylamine, or butylamine. The mono-nitration can be achieved by a reaction of perylene bisimides (**3a**–**3c**) with cerium (IV) ammonium nitrate (CAN) and HNO_3 (or H_2SO_4) under ambient temperature for 2 h, giving **2a**–**2c** in high yields of ca. 90%. The reduction of nitroperylene bisimides (**2a**–**2c**) by tin (II) chloride dihydrate ($SnCl_2 \cdot 2H_2O$) in refluxing THF obtained the corresponding 1-aminoperylene bisimides **1a**–**1c**. The presence of a single amino substituent can be verified by the presence of a signal at δ 5.1 ppm ($-NH_2$) in ^{1}H NMR spectrum and the absorption at 3343 and 3240 cm^{-1} in FT-IR spectrum, corresponding to the stretching of the primary amino group (Fig. 2). In addition, the nucleophilic

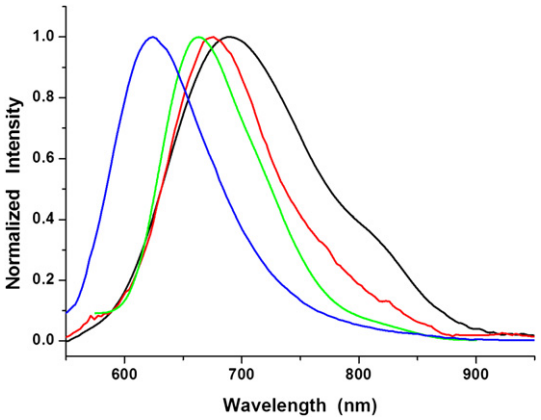

Fig. 4. Normalized emission spectra of **1a** in cyclohexane (blue line) ethyl acetate (green line), dichloromethane (red line) and acetonitrile (black line).

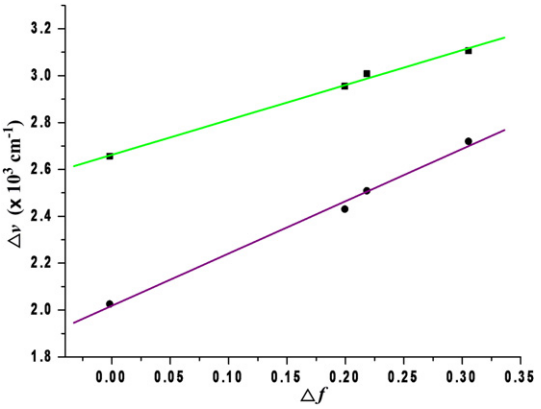

Fig. 5. Lippert–Mataga plots for **1a** (purple line) and **5a** (green line). The solvents are (1) cyclohexane, (2) ethyl acetate, (3) dichloromethane, (4) acetonitrile.

substitution of 1-bromoperylene bisimide (**6a**) with piperidine at 60 °C [33] afforded the corresponding monopiperidinyl bisimide (**5a**) as a deep green solid.

3.2. Photophysical properties of dyes

Fig. 3 shows the steady state absorption spectra of the purple dye **1a**, the red dye **2a**, and the green dye **5a** in dichloromethane. The spectra of **1b** and **1c** can be found in the Supplementary data. The spectrum of **1a** is dominated by a very broad, and nearly structureless, absorption band that spans a large part of the visible spectrum (380–740 nm). This broad absorption band is red-shifted relative to that of **2a**, but it is blue-shifted relative to that of **5a** (390–760 nm). The main differences between the spectra are the absorption near 422 and 566 nm for **1a** and the peaks at 445 and 607 nm in the spectrum of **5a**. These two features account for the large differences in color observed by the naked eye. Moreover, the longest wavelength absorption band of **1a**–**1c** and **5a** exhibits a red shift upon increasing the solvent polarity (Tables 1 and 2 and Supplementary data), which is consistent with the previous studies [31].

Table 3
Calculated and experimental parameters for perylene diimide derivatives **1a**–**1c** and **5a**–**5c**.

Compound	HOMO[a]	LUMO[a]	E_g[a]	E_g[b]	Twisting angle (°)
1a	−5.62	−3.21	2.41	2.24	9.23, 17.49
1b	−5.65	−3.24	2.41	2.24	9.16, 17.57
1c	−5.65	−3.25	2.40	2.25	9.19, 17.50
5a	−5.54	−3.21	2.33	2.13	10.07, 18.03
5b[c]	−5.42	−3.14	2.28	2.12	10.11, 18.46
5c[c]	−5.41	−3.13	2.28	2.12	10.24, 18.22

[a] Calculated by DFT/B3LYP (in eV).
[b] At absorption maxima ($E_g = 1240/\lambda_{max}$, in eV).
[c] Reference [33].

The fluorescence spectra of **1a** in various solvents are shown in Fig. 4 and summarized in Table 1; the fluorescence spectra of **1b**–**1c** can be found in the Supplementary data. The fluorescence spectra shift significantly to the red upon increasing solvent polarity, indicating strong intramolecular charge transfer (ICT) characteristics for the excited states of **1a**–**1c**. Using the well-established fluorescence solvatochromic shift method [34], we measured the stabilization of the excited states of **1a** and compared these results to those of **5a** (Table 2). The emission λ_{max} of each compound was measured in four solvents with dielectric constants ranging from 2.02 to 37.50. The solvent polarity-dependent emission can be expressed quantitatively derived from dielectric polarization, specifying that the spectra shifts of the fluorescence upon increasing the solvent polarity depend on the difference in permanent dipole moments between ground ($\overrightarrow{\mu_g}$) and excited ($\overrightarrow{\mu_e}$) state [35]. The change of magnitudes for dipole moments between ground and excited states, *i.e.*, $\Delta\mu = |\overrightarrow{\mu_e} - \overrightarrow{\mu_g}|$, can be calculated by the Lippert–Mataga equation and expressed as:

$$\bar{\nu}_a - \bar{\nu}_f = \frac{2}{hc}\left(\mu_e - \mu_g\right)^2 a_0^{-3}\Delta f + \text{const.} \quad (1)$$

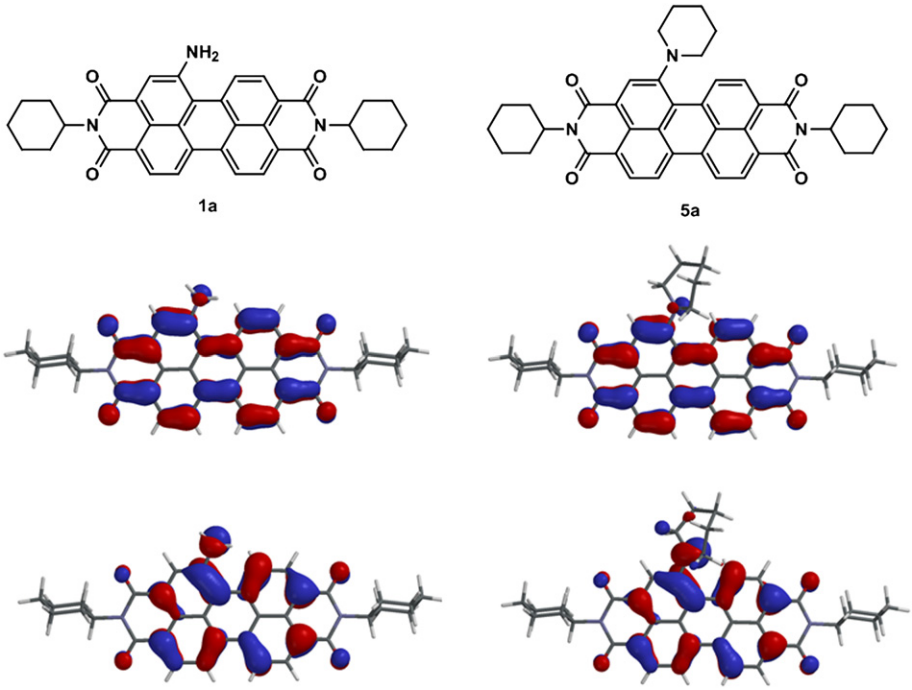

Fig. 6. Computed frontier orbitals of **1a** and **5a**. The upper graphs are the LUMOs and the lower ones are the HOMOs.

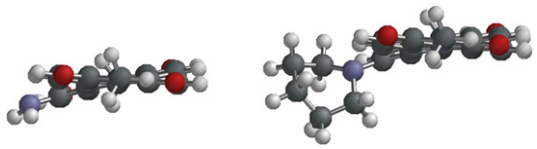

Fig. 7. DFT (B3LYP/6-31G**) geometry-optimized structures of **1a** (left) and **5a** (right) shown with view along the long axis. For computational purposes, methyl groups replace the cyclohexyl groups at the imide positions.

where h is the Planck constant, c is the speed of light, and a_0 denotes the cavity radius in which the solute resides, calculated to be 7.0 Å via Hartree–Fock theories with 6-31G (d′, p′) basis, $\bar{\upsilon}_a - \bar{\upsilon}_f$ is the Stokes shift of the absorption and emission peak maximum, and Δf is the orientation polarizability defined as:

$$\Delta f = f(\varepsilon) - f\left(n^2\right) = \frac{\varepsilon - 1}{2\varepsilon + 1} - \frac{n^2 - 1}{2n^2 + 1} \quad (2)$$

The plot of the Stokes shift $\bar{\upsilon}_a - \bar{\upsilon}_f$ as a function of Δf is sufficiently linear for **1a** and **5a** (Fig. 5). Accordingly, $\Delta\mu = |\overrightarrow{\mu_e} - \overrightarrow{\mu_g}|$ was deduced to be 7.4 D and 7.1 D for **1a** and **5a**, respectively. These values of $\Delta\mu$ are very close to that determined for alkylamino-substituted perylene bisimides [31].

3.3. Quantum chemistry computation

To gain insight into the electronic properties of **1a**–**1c** and **5a**–**5c**, quantum chemical calculations were performed using density functional theory (DFT) at the B3LYP/6-31G** level [37]. Fig. 6 shows the highest occupied molecular orbital (HOMO) and the lowest unoccupied molecular orbital (LUMO) of **1a** and **5a**. The HOMO of both **1a** and **5a** is delocalized mainly on the amino group and the perylene core, while the LUMO is extended from the central perylene core to the bisimide groups. The calculated and experimental parameters are summarized in Table 3. The results indicate that both the HOMO and LUMO energy levels of **1a**–**1c** are similar to those of **5a**–**5c**. Furthermore, DFT (B3LYP/6-31G**) calculations show that the ground-state geometries of the perylene core have two core twist angles, *i.e.*, approximate dihedral angles between the two naphthalene subunits attached to the central benzene ring; these are ~9° and ~17° for **1a**–**1c** and 10° and 18° for **5a**–**5c** (Table 3 and Fig. 7). As a whole, the core twist angles of primary amino-substituted perylene bisimides (**1a**–**1c**) are smaller than those of sterically bulky piperidinyl-substituted perylene bisimides (**5a**–**5c**).

Table 4
Summary of half-wave redox potentials, HOMO and LUMO energy levels for **1a**–**1c** and **5a**.

Compound	$E^{+}{}_{1/2}$[a]	$E^{2+}{}_{1/2}$[a]	$E^{-}{}_{1/2}$[a]	$E^{2-}{}_{1/2}$[a]	E_{HOMO}/E_{LUMO} (eV)[b]
1a	0.97	1.36	−0.97	−1.09	−5.57/−3.33
1b	0.99	1.38	−0.96	−1.08	−5.59/−3.35
1c	1.00	1.39	−0.96	−1.07	−5.60/−3.35
5a	0.82	1.32	−0.98	−1.15	−5.44/−3.31

[a] Measured in a solution of 0.1 M tetrabutylammonium hexafluorophosphate (TBAPF6) in dichloromethane versus SCE (in V).
[b] Calculated from $E_{HOMO} = -4.88 - (E_{oxd} - E_{Fc/Fc+})$, $E_{LUMO} = E_{HOMO} + E_g$.

3.4. Electrochemical properties of dyes

Fig. 8 shows that the cyclic voltammograms of **1a** and **5a** undergo two quasi-reversible one-electron oxidations and two quasi-reversible one-electron reductions in dichloromethane at modest potentials. Table 4 summarizes the redox potentials and the HOMO and LUMO energy levels estimated from cyclic voltammetry (CV) for **1a**–**1c** and **5a** [38]. It appears that the first oxidation potential of **5a** is smaller than those of **1a**–**1c**; this can be explained by the fact that the piperidinyl substituent has better electron-donating ability than the amino substituent. The HOMO and LUMO energy levels of **1a**–**1c** (**5a**) are estimated in the range of −5.57 to −5.60 (−5.44) eV and −3.33 to −3.35 (−3.31) eV, respectively. As expected, the HOMO–LUMO energy gap of **5a** is

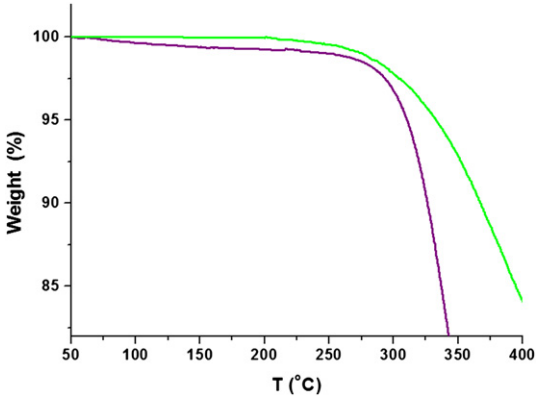

Fig. 9. Thermogravimetric analysis graphs for **1a** (purple line) and **5a** (green line) in nitrogen atmosphere at normal pressure. Heating rate, 10 °C/min.

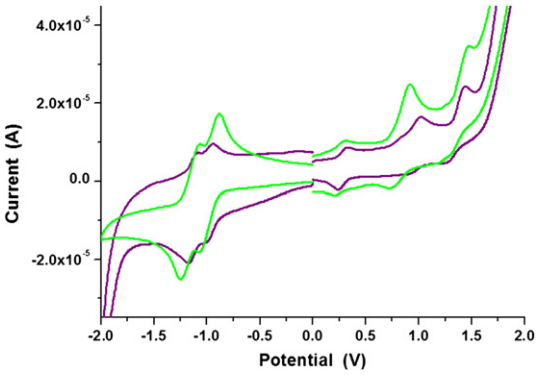

Fig. 8. The cyclic voltammograms of **1a** (purple line) and **5a** (green line) measured in dichloromethane solution with ferrocenium/ferrocene, at 200 mV/s.

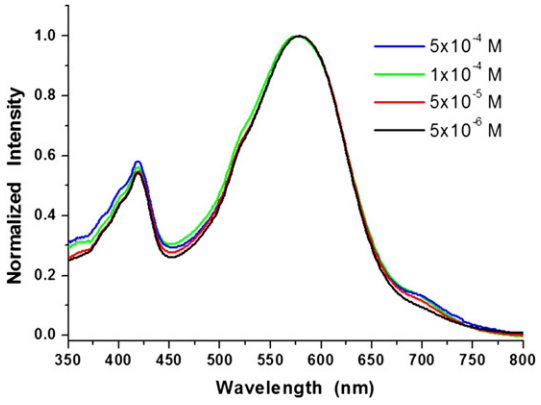

Fig. 10. Normalized absorption spectra of **1a** at different concentrations in ethyl acetate.

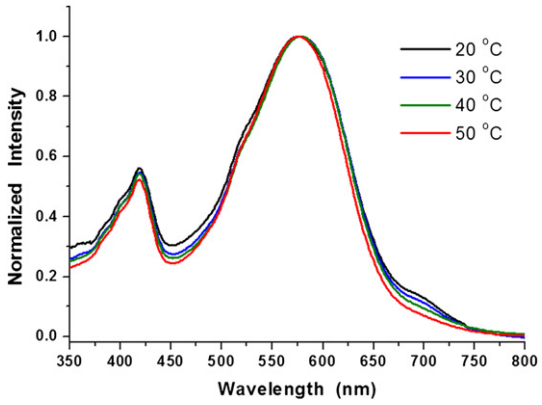

Fig. 11. Normalized absorption spectra of **1a** at different temperatures in ethyl acetate.

smaller than those of **1a**–**1c**, which is in good agreement with the theoretical calculations.

3.5. Thermal properties of dyes

The thermal properties of **1a**–**1c** and **5a** were investigated by thermogravimetric analysis (TGA) and differential scanning calorimetry (DSC). Thermogravimetric analyses revealed that **1a**–**1c** and **5a** were thermally stable materials, and that the onset of decomposition temperatures occurred above 300 °C under nitrogen (Fig. 9). Several perylene bisimide derivatives having long alkyl chains are liquid crystalline (LC) [39]. However, according to DSC analyses these compounds had no observable liquid crystalline transitions between −50 and 300 °C.

3.6. Influence of concentration and temperature on the aggregation behaviors of dyes

The stacking behaviors of **1a**–**1c** in methylcyclohexane (MCH), dichloromethane, and ethyl acetate were investigated by concentration-dependent UV–Vis measurements (from 10^{-4} M to 10^{-6} M). Fig. 10 shows the absorption spectra of **1a** at different concentrations in ethyl acetate; those of **1b**–**1c** can be found in the Supplementary data. At high concentrations, J-type stacks are formed (~700 nm), whereas at low concentrations, the spectrum is similar to the one in dichloromethane where no stacking takes place (Supplementary data). Due to the low solubility of **1a**–**1c** in MCH (highest concentration is approximately 10^{-5} M), no concentration-dependent UV–Vis measurements were performed. The stacking behaviors of **1a**–**1c** in ethyl acetate were further investigated by temperature-dependent UV–vis measurements (from 20 to 50 °C). Upon cooling, a clear red shift was observed in the UV–vis measurements for all perylene bisimides **1a**–**1c**, indicating the formation of J-type aggregates (Fig. 11 and Supplementary data).

4. Conclusions

We have successfully synthesized a series of purple dyes based on amino-substituted perylene bisimides, *i.e.*, 1-aminoperylene bisimides (**1a**–**1c**). These molecules undergo an excited-state intramolecular electron transfer (ESIET) reaction, resulting in a unique charge transfer emission, of which the peak wavelength exhibit strong solvatochromism. They undergo two quasi-reversible one-electron oxidations and two quasi-reversible one-electron reductions in dichloromethane at modest potentials. In addition, compounds **1a**–**1c** display good thermal stability as well as good optical stability and reversible redox properties. Working toward their applications on photoactive charge transport materials is in progress.

Acknowledgement

Financial support from the National Science Council of the Republic of China is gratefully acknowledged (NSC 99-2113-M-035-001-MY2).

Appendix. Supplementary data

Supplementary data (^{1}H NMR spectra of **1a**–**1c** and **5a**; absorption and emission spectra of **1b** and **1c** in various conditions; absorption spectra of **1a** at different concentrations in dichloromethane) associated with this article can be found, in the online version, at doi:10.1016/j.dyepig.2011.06.023.

References

[1] Dentani T, Funabiki K, Jin JY, Yoshida T, Minoura H, Matsui M. Application of 9-substituted 3,4-perylenedicarboxylic anhydrides as sensitizers for zinc oxide solar cell. Dyes and Pigments 2007;72:303–7.
[2] Dinçalp H, Aşkar Z, Zafer C, İçli S. Effect of side chain substituents on the electron injection abilities of unsymmetrical perylene diimide dyes. Dyes and Pigments 2011;91:182–91.
[3] Li J, Dierschke F, Wu J, Grimsdale AC, Müllen K. Poly(2,7-carbazole) and perylene tetracarboxydiimide: a promising donor/acceptor pair for polymer solar cells. Journal of Materials Chemistry 2006;16:96–100.
[4] Shibano Y, Umeyama T, Matano Y, Imahori H. Electron-donating perylene tetracarboxylic acids for dye-sensitized solar cells. Organic Letters 2007;9:1971–4.
[5] Tian H, Liu PH, Zhu W, Gao E, Wu DJ, Cai S. Synthesis of novel multi-chromophoric soluble perylene derivatives and their photosensitizing properties with wide spectral response for SnO_2 nanoporous electrode. Journal of Materials Chemistry 2000;10:2708–15.
[6] Tang CW. Two-layer organic photovoltaic cell. Applied Physics Letters 1986;48:183–5.
[7] Wang HY, Peng B, Wei W. Solar cells based on perylene bisimide derivatives. Progress in Chemistry 2008;20:1751–60.
[8] Huang C, Barlow S, Marder SR. Perylene-3,4,9,10-tetracarboxylic acid diimides: synthesis, physical properties, and use in organic electronics. Journal of Organic Chemistry 2011;76:2386–407.
[9] Li X, Sinks LE, Rybtchinski B, Wasielewski MR. Ultrafast aggregate-to-aggregate energy transfer within self-assembled light-harvesting columns of zinc phthalocyanine tetrakis(perylenediimide). Journal of the American Chemical Society 2004;126:10810–1.
[10] Rybtchinski B, Sinks LE, Wasielewski MR. Combining light-harvesting and charge separation in a self-assembled artificial photosynthetic system based on perylenediimide chromophores. Journal of the American Chemical Society 2004;126:12268–9.
[11] Matsui M, Wang M, Funabiki K, Hayakawa Y, Kitaguchi T. Properties of novel perylene-3,4:9,10-tetracarboxidiimide-centred dendrimers and their application as emitters in organic electroluminescence devices. Dyes and Pigments 2007;74:169–75.
[12] Würthner F, Stolte M. Naphthalene and perylene diimides for organic transistors. Chemical Communications 2011;47:5109–15.
[13] Reghu RR, Bisoyi HK, Grazulevicius JV, Anjukandi P, Gaidelis V, Jankauskas V. Air stable electron-transporting and ambipolar bay substituted perylene bisimides. Journal of Materials Chemistry 2011;21:7811–9.
[14] Kim FS, Guo X, Watson MD, Jenekhe SA. High-mobility ambipolar transistors and high-gain inverters from a donor-acceptor copolymer semiconductor. Advanced Materials 2009;21:1–5.
[15] Zaumseil J, Sirringhaus H. Electron and ambipolar transport in organic field-effect transistors. Chemical Reviews 2007;107:1296–323.
[16] Locklin J, Li D, Mannsfeld SCB, Borkent EJ, Meng H, Advincula R, et al. Organic thin film transistors based on cyclohexyl-substituted organic semiconductors. Chemistry of Materials 2005;17:3366–74.
[17] Jones BA, Ahrens MJ, Yoon MH, Facchetti A, Marks TJ, Wasielewski MR. High-mobility air-stable n-type semiconductors with processing versatility: dicyanoperylene-3,4:9,10-bis(dicarboximides). Angewandte Chemie International Edition 2004;43:6363–6.
[18] Tan W, Li X, Zhang J, Tian H. A photochromic diarylethene dyad based on perylene diimide. Dyes and Pigments 2011;89:260–5.
[19] Sakong C, Kim YD, Choi JH, Yoon C, Kim JP. The synthesis of thermally-stable red dyes for LCD color filters and analysis of their aggregation and spectral properties. Dyes and Pigments 2011;88:166–73.

[20] Zhao Y, Wasielewski MR. 3,4:9,10-Perylenebis(dicarboximide) chromophores that function as both electron donors and acceptors. Tetrahedron Letters 1999;40:7047–50.
[21] Rohr U, Kohl C, Müllen K, Van de Craats A, Warman J. Liquid crystalline coronene derivatives. Journal of Materials Chemistry 2001;11:1789–99.
[22] Zhao C, Zhang Y, Li R, Li X, Jiang J. Di(alkoxy)- and di(alkylthio)-substituted perylene-3,4;9,10-tetracarboxy diimides with tunable electrochemical and photophysical properties. Journal of Organic Chemistry 2007;72:2402–10.
[23] Chao CC, Leung MK. Photophysical and electrochemical properties of 1,7-diaryl-substituted perylene diimides. Journal of Organic Chemistry 2005;70:4323–31.
[24] Weitz RT, Amsharov K, Zschieschang U, Villas EB, Goswami DK, Burghard M, et al. Organic n-channel transistors based on core-cyanated perylene carboxylic diimide derivatives. Journal of the American Chemical Society 2008;130:4637–45.
[25] Chen KY, Chow TJ. 1,7-Dinitroperylene bisimides: facile synthesis and characterization as n-type organic semiconductors. Tetrahedron Letters 2010;51:5959–63.
[26] Fan L, Xu Y, Tian H. 1,6-Disubstituted perylene bisimides: concise synthesis and characterization as near-infrared fluorescent dyes. Tetrahedron Letters 2005;46:4443–7.
[27] Jones BA, Facchetti A, Wasielewski MR, Marks TJ. Tuning orbital energetics in arylene diimide semiconductors. Materials design for ambient stability of n-type charge transport. Journal of the American Chemical Society 2007;129:15259–78.
[28] Chen HZ, Ling MM, Mo X, Shi MM, Wang M, Bao Z. Air stable n-channel organic semiconductors for thin film transistors based on fluorinated derivatives of perylene diimides. Chemistry of Materials 2007;19:816–24.
[29] Sandrai M, Hadel L, Sauers RR, Husain S, Krogh-Jespersen K, Westbrook JD, et al. Lasing action in a family of perylene derivatives: singlet absorption and emission spectra, triplet absorption and oxygen quenching constants, and molecular mechanics and semiempirical molecular orbital calculations. Journal of Physical Chemistry 1992;96:7988–96.
[30] Ahrens MJ, Sinks LE, Rybtchinski B, Liu W, Jones BA, Giaimo JM, et al. Self-assembly of supramolecular light-harvesting arrays from covalent multi-chromophore perylene-3,4:9,10-bis(dicarboximide) building blocks. Journal of the American Chemical Society 2004;126:8284–94.
[31] Ahrens MJ, Tauber MJ, Wasielewski MR. Bis(n-octylamino)perylene-3,4:9,10-bis(dicarboximide)s and their radical cations: synthesis, electrochemistry, and ENDOR spectroscopy. Journal of Organic Chemistry 2006;71:2107–14.
[32] Alvino A, Franceschin M, Cefaro C, Borioni S, Ortaggi G, Bianco A. Synthesis and spectroscopic properties of highly water-soluble perylene derivatives. Tetrahedron 2007;63:7858–65.
[33] Rajasingh P, Cohen R, Shirman E, Shimon LJW, Rybtchinski B. Selective bromination of perylene diimides under mild conditions. Journal of Organic Chemistry 2007;72:5973–9.
[34] Lakowicz JR. Principles of fluorescence spectroscopy. 2nd ed. New York: Plenum; 1999.
[35] Chen KY, Hsieh CC, Cheng YM, Lai CH, Chou PT, Chow TJ. Tuning excited-state electron transfer from an adiabatic to nonadiabatic type in donor-bridge-acceptor systems and the associated energy-transfer process. Journal of Physical Chemistry A 2006;110:12136–44.
[36] Würthner F. Perylene bisimide dyes as versatile building blocks for functional supramolecular architectures. Chemical Communication 2004;14:1564–79.
[37] González SR, Casado J, Navarrete JTL, Blanco R, Segura JL. A β-naphthaleneimide-modified terthiophene exhibiting charge transfer and polarization through the short molecular axis. Joint spectroscopic and theoretical study. Journal of Physical Chemistry A 2008;112:6732–40.
[38] Oh SH, Kim BG, Yun SJ, Maheswara M, Kim K, Do JY. The synthesis of symmetric and asymmetric perylene derivatives and their optical properties. Dyes and Pigments 2010;85:37–42.
[39] van Herrikhuyzen J, Syamakumari A, Schenning APHJ, Meijer EW. Synthesis of n-type perylene bisimide derivatives and their orthogonal self-assembly with p-type oligo(p-phenylene vinylene)s. Journal of the American Chemical Society 2004;126:10021–7.